Assessing the Impact of Meteorological Parameters and Topography on Radioactive Plume Dispersion: A Simulation Study Using the HotSpot Model

YASSINE EL KHADIRI*, OUADIE KABACH*, ANAS OTMANI, ABDESLAM LACHHAB, EL MAHJOUB CHAKIR

LPMS, faculty of sciences, Ibn Tofail University, Kenitra, Morocco.

* Corresponding authors' email addresses: yassine.elkhadiri@uit.ac.ma (Yassine El Khadiri); ouadie.kabach10@gmail.com (Ouadie Kabach)

Abstract

Nuclear and radiological materials, essential in various sectors, pose significant risks if misused for terrorism. The detonation of a radiological dispersal device (RDD) can have catastrophic consequences. This study examines how meteorological parameters and topography affect the dispersion of radioactive clouds from an RDD attack using the HotSpot model. Simulations were based on a hypothetical scenario involving a radioactive source at a football stadium renovation site. The study assesses wind speed, atmospheric stability, and precipitation's impact on plume dispersion and ground contamination. Results highlight the crucial role of these factors in determining the extent and severity of radiological contamination, providing essential insights for risk management and emergency planning.

Keywords: Radiological Dispersal Device; Plume Dispersion; Meteorological Parameters; Ground Contamination; HotSpot Model.

1. Introduction

Nuclear and radiological materials have demonstrated their utility for our societies in medicine, agriculture, industry, and energy. However, there is a risk that they could be used for terrorist purposes or to commit other criminal acts. The detonation of an improvised nuclear device (IND) a radiological dispersal device (RDD), or the installation of a radiological exposure device (RED), can have disastrous consequences. Such attacks would have harmful effects on human health and the environment, cause panic, and impact economic and political stability [1].

To date, a "dirty bomb" has never exploded, but several cases indicate that attacks have been planned and prepared. The primary challenge for terrorists is acquiring the radioactive materials to include in the bomb. Radioactive materials can come from an abandoned ("orphan") source, as in Goiania, be stolen from a facility where they are legally used, or be purchased by terrorists posing as legitimate users or on the black market. In practice, availability will likely be limited to radionuclides used for peaceful purposes in industry, research, or medicine [1–4]. Radioactive sources with high activities that are widely available are probably of particular interest to terrorists (see Table 1). Consequently, the list of radionuclides of concern that should be considered in potential dirty bomb scenarios may be quite short.

In particular, cesium chloride (CsCl) in powder form seems well-suited for being dispersed into a cloud of fine dust and widely spread, making it a likely choice for creating an area denial

effect—causing a level of contamination that would trigger the quarantine of an area and necessitate extensive large-scale cleanup [5,6]. This is likely why scenarios involving radiological attacks with this radionuclide have received significant attention. Besides the radioactive contamination of surfaces and infrastructure with a marked economic impact, the short- and long-term health effects on victims near the detonation point must also be considered.

Tabel 1. Likely radioactive sources for a dirty bomb construction [5].

Radionuclide	Source	Activity (Ci)
Cs-137		
Radiation: β, γ	Calibration irradiator	Up to 2200
$T_{1/2\ Phys}$: 30.1 years	Blood irradiator	2000 - 7000 (typically 3000)
$T_{1/2\ eff.}$: 109 days	Research irradiator	Up to 20,000
Powder, salt (CsCl)		
Co-60		
Radiation: β, γ	Teletherapy	1000 - 15,000
$T_{1/2\ Phys}$: 5.3 years	Gamma knife	6000 - 7000
$T_{1/2\ eff.}$: 1.6 years	Panoramic irradiator	1,000,000 - 7,000,000
Metal		
Sr-90		
Radiation: β		
$T_{1/2\ Phys}$: 28.2 years	Radioisotope thermoelectric generator	20,000 - 250,000
$T_{1/2\ eff.}$: 4.6 years		
Ceramic ($SrTiO_3$)		
Ir-92		
Radiation: β, γ		
$T_{1/2\ Phys}$: 73.8 days	Industrial radiography source	up to 1500
$T_{1/2\ eff.}$: not available		
Metal		
Pu-238		
Radiation: α, γ	Radioisotope thermoelectric generator	up to 150,000
$T_{1/2\ Phys}$: 87.7 years		
$T_{1/2\ eff.}$: 50 years		
Ceramic (PuO_2)		
Am-241		
Radiation: α, γ	Well logging source	15 - 30
$T_{1/2\ Phys}$: 432.7 years	Smoke detectors	10 - 6
$T_{1/2\ eff.}$: 45 years		
Pressed ceramic powder (AmO_2)		
Cf-252		
Radiation: α, neutron		
$T_{1/2\ Phys}$: 2.65 years	Well logging source	2.5
$T_{1/2\ eff.}$: 2.5 years		
Ceramic (Cf_2O_3)		

In this article, we will study the influence of meteorological parameters and topography on the dispersion of the radioactive cloud following a malicious act involving an RDD device. We will primarily evaluate the impact on variations in ground deposition surfaces, plume exposure, and TEDE (Total Effective Dose Equivalent) values. This work will also examine the influence of meteorological parameters and topography on the dispersion of the radioactive cloud resulting from a malicious act involving nuclear or radiological materials. We will mainly assess the impact on variations in ground deposition surfaces, plume exposure, and TEDE values. The approach involves conducting several simulations using the Hotspot model, based on a malicious act scenario involving a radioactive source located at the renovation site of a

football stadium while varying meteorological conditions. The choice of a football stadium as the scenario site is particularly significant in our study. Football stadiums are often frequented by large numbers of people, significantly increasing the potential impact of a malicious act involving nuclear or radiological materials. Due to their open design and crowd density during sporting events, stadiums represent potential targets for attacks aiming to cause extensive damage, sow panic, and generate severe health and environmental consequences. By choosing a football stadium as the scenario, our study aims to realistically assess the repercussions of a malicious act in a highly populated public place, providing meaningful results for risk management and emergency planning [5,7–11].

2. Models, Data, Methodology

2.1. Scenario of a malicious act involving a radioactive source

In this hypothetical scenario, terrorists have selected the day of a highly publicized football match between two major teams in a derby to carry out a radiological attack. The stadium, neutral ground not associated with either team, is filled with a large crowd of spectators. Situated near the city's urban forest, a popular fast-food restaurant, a new residential area, and approximately 2.5 km from the highway entry, the stadium is in a bustling area. The terrorists have discreetly placed an RDD in a suspicious vehicle parked at a construction site involved in the stadium's renovation. Upon detonation, the device causes an explosion, dispersing radioactive material and exposing many spectators, as well as individuals at the construction site, to dangerous levels of radiation.

Figure 1. Example of a dirty bomb: radiological dispersal device using explosive [12].

2.2. Data related to the source

In this scenario, a quantity of 74 TBq of Cs-137 is involved in the dispersion of the plume following the use of an explosive amount equivalent to 1 lb. of TNT. In our study, TEDE thresholds are defined by the following contours: red contour (0.01 Sv), green contour (0.001 Sv), and blue contour (0.0001 Sv). The ground deposition thresholds are established with the following contours: red (300 kBq/m²), green (30 kBq/m²), and blue (3 kBq/m²). The model parameters include an Airborne Release Fraction (ARF= 0.01), an Aerodynamic Median Activity Diameter (AMAD=1 µm), a Respirable Fraction (RF=1), a deposition velocity of 0.3 cm/s, a Damage Ratio (DR=1), a Leak Path Factor (LPF=1), an average receptor height of 1.5 m, an average human breathing rate of 4.17 x 10^{-4} m³/s (ICRP 66, 1994), and dose conversion factors following the FGR13 library [13,14].

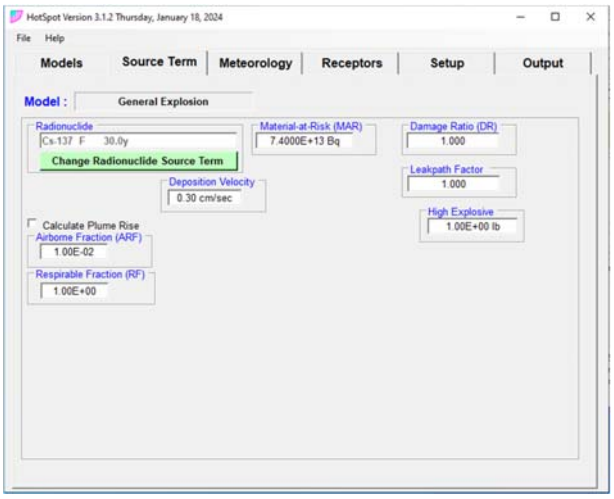

Figure 2. Source term definition.

2.3. Dispersion model analysis

The NARAC HotSpot code from the United States has been selected to comprehensively evaluate a potential dirty bomb scenario [10,15]. This tool offers several key advantages for radiological emergency response:

- Dispersion modeling: it accurately simulates the dispersion of radioactive material resulting from an explosion.
- Contamination display: it presents contamination levels in units familiar to emergency responders, facilitating swift decision-making.
- Graphical output: the code provides a visual representation of the contaminated area and calculates contamination levels within this zone.
- Preventive actions: it supports the implementation of preventive measures and countermeasures in emergency preparedness and response systems.
- Quantitative guidance: the code produces quantitative outputs that can guide the deployment of radiological protection experts and aid in making specific emergency management decisions during a radiological release.

While the HotSpot code is reliable for distances up to 10 km, results beyond this range should be analyzed with caution. Despite this limitation, the code remains a crucial tool for both immediate response and long-term planning in radiological emergencies.

HotSpot relies on the Gaussian dispersion model, a widely used and validated approach within the scientific community for initial atmospheric dispersion calculations. This model typically aligns well with experimental data and is included in many governmental guidelines, being also recognized by the Environmental Protection Agency. Figure 3 illustrates the Gaussian model diagram utilized in the HotSpot code in the case of an RDD device to determine the concentration of radioactive material in the air.

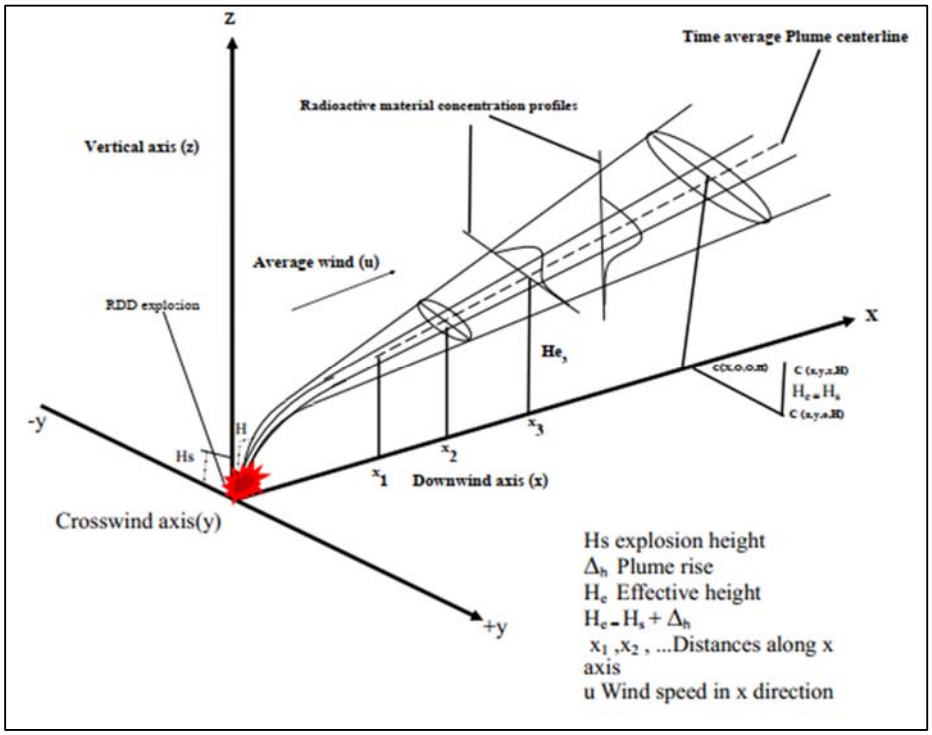

Figure 3. Geometry of a Gaussian plume in case of an RDD.

The Gaussian model equation used in HotSpot to determine the time-integrated atmospheric concentration of radioactive material at any point in space is:

$$C(x, y, e, H) = \frac{Q}{2\pi\sigma_x\sigma_y} \exp\left[-\frac{1}{2}\left(\frac{y}{\sigma_y}\right)^2\right]\left\{\exp\left[-\frac{1}{2}\left(\frac{z-H}{\sigma_z}\right)^2\right] + \exp\left[-\frac{1}{2}\left(\frac{z+H}{\sigma_z}\right)^2\right]\right\}\exp\left[-\frac{\lambda x}{u}\right] \qquad (1)$$

Where: c represents the time-integrated atmospheric concentration of the radionuclide ($Bq \cdot s/m^3$), Q is the source term (Bq), H is the effective release height (m), λ is the radioactive decay constant (s^{-1}), x is the downwind distance (m), y is the crosswind distance (m), z is the vertical distance (m), σ_y is the standard deviation of the downwind concentration distribution (m), σ_y is the standard deviation of the crosswind concentration distribution (m), σ_z is the standard deviation of the vertical concentration distribution (m), and u is the wind speed (m/s). HotSpot assumes the target individual remains at the same downwind location during the plume passage and defaults to a 10-minute release duration for radioactive material. The improved Briggs formula allows calculations from 0.1 km up to 10 km, with possible extensions to 20 or 30 km, although Briggs advises against such extensions without additional validation. Despite this, the formulae are often used up to 100 km. In modeling the initial distribution of material from a dirty bomb explosion, HotSpot assumes five separate source zones (h(1) to h(5)) along the vertical axis of the explosion, each represented by two virtual source points upstream of the actual explosion point (see Figure 4). Initial dispersion coefficients are estimated as follows:

- Sigma-y: 50% of the cloud radius.

- Sigma-z: 20% of the cloud height.

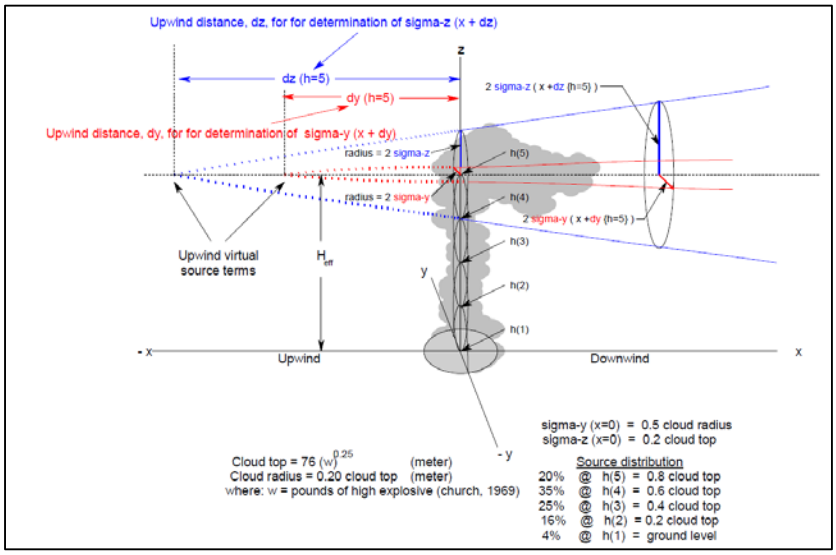

Figure 4. Virtual source terms used by the Hotspot model to simulate the initial distribution of the dispersed cloud following a dirty bomb explosion.

Distances dy and dz are calculated using Briggs' formulation. The cloud top height is determined based on the explosive amount (w) using the equation:

$$\text{Cloud top} = 76\,(2.2\,w)^{0.25} \tag{2}$$

Where w is the explosive quantity in kg. The cloud radius is given by:

$$R = 0.2\ \text{Cloud top} \tag{3}$$

The effective height is calculated using:

$$H_{eff} = 0.8\ \text{Cloud top} \tag{4}$$

2.4. Meteorological conditions at the site of the malicious act

The climatic conditions of Kenitra are characterized by relatively consistent wind speeds and highly variable precipitation throughout the year. The average wind speed hovers between 3 to 5 meters per second, representing minor fluctuations with slightly higher speeds in the winter months and a dip during the summer. The wind speed probabilities are as follows: 0 to 2 m/s occur infrequently, primarily during calm periods; 2 to 5 m/s is the most common range, reflecting the typical breezy conditions; and 5 to 10 m/s are less frequent but occur during windy conditions, particularly in the transitional seasons of spring and autumn.

On the other hand, precipitation patterns show a stark contrast, with the highest rainfall occurring from January to March, where monthly totals can reach up to 100 mm. This period also sees the most precipitation days, often exceeding 10 days per month. In stark contrast, the summer months from April to August are notably dry, with precipitation rarely exceeding 10 mm per month and fewer than 5 rainy days. The rainfall picks up again in autumn, particularly in November, which mirrors the winter pattern with significant precipitation. This analysis highlights the seasonal variability in Kenitra, with a marked distinction between the wet winters and dry summers, essential for planning in sectors such as agriculture, water resource

management, and urban planning. Figure 5. Show monthly distribution of wind direction, wind speed, precipitation, and number of precipitation days.

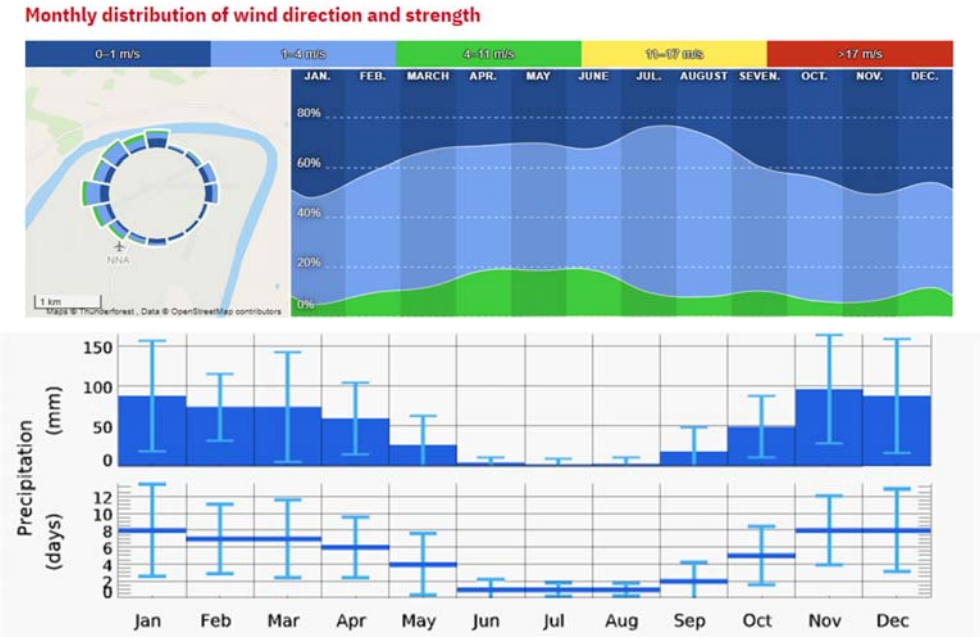

Figure 5. Monthly distribution of wind direction, wind speed, precipitation (mm), and number of precipitation days [16].

3. Results and discussion

As previously mentioned, in this scenario, an amount of 74 TBq of the radioactive source Cs-137 is involved in the dispersion of the plume following the use of an explosive amount equivalent to 1 lb of TNT. In our study, the Total Effective Dose Equivalent (TEDE) thresholds are defined with a red contour (0.01 Sv), a green contour (0.001 Sv), and a blue contour (0.0001 Sv), while the ground deposition thresholds are established with a red contour (300 kBq/m²), a green contour (30 kBq/m²), and a blue contour (3 kBq/m²). Additionally, different weather conditions affect the dispersion of the plume. Wind speed is considered at 10 m above the ground, ranging from light wind (2 m/s) to medium (5 m/s) and strong (10 m/s). Stability classes are determined according to the Pasquill classification, using stable (F), slightly unstable (C), and very unstable (A) stability cases. Atmospheric stability classes are defined based on turbulence conditions and atmospheric stratification. The stable class (F) is characterized by low turbulence and strong atmospheric stratification, often observed in anticyclonic conditions with a clear sky and low wind. The slightly unstable class (C) is associated with moderate turbulence and weaker atmospheric stratification, generally observed under a partly cloudy sky with moderate wind. Finally, the very unstable class (A) is marked by high turbulence and weak atmospheric stratification, commonly observed during periods of strong sunlight and variable winds. To assess the impact of precipitation on the evolution of the radioactive cloud, particularly on ground deposition, plume exposure, and TEDE values, we conducted several simulations by introducing the "precipitation" parameter with different rates (1 mm/h, 5 mm/h, and 10 mm/h) for slightly unstable (C) and very unstable (A) stability classes.

The following figures illustrate the impact of the explosion. One important initial observation is the absence of a red contour (interior) in terms of TEDE according to the defined thresholds in our scenario. Atmospheric stability, under dry conditions and with a low wind

speed of 2 m/s, leads to the expansion of the green zone radius of the plume while shortening the distance of the blue zone contour, thus affecting ground deposition areas. For the stability class F, the green zone in terms of TEDE is 1E-3 km², while for class C, it reaches 2E-3 km². Increasing the speed reduces the radius of the plume zone. For distances close to the explosion, significant TEDE values are observed when there is slight atmospheric instability (class C) and low wind. Furthermore, wind speed affects the ground deposition area. For example, at a wind speed of 2 m/s in slightly unstable atmospheric conditions (class C), the red zone is 7E-3 km² and the green zone is 0.57 km². At a wind speed of 10 m/s, the red zone decreases to 5E-3 km², while the green zone is 0.085 km².

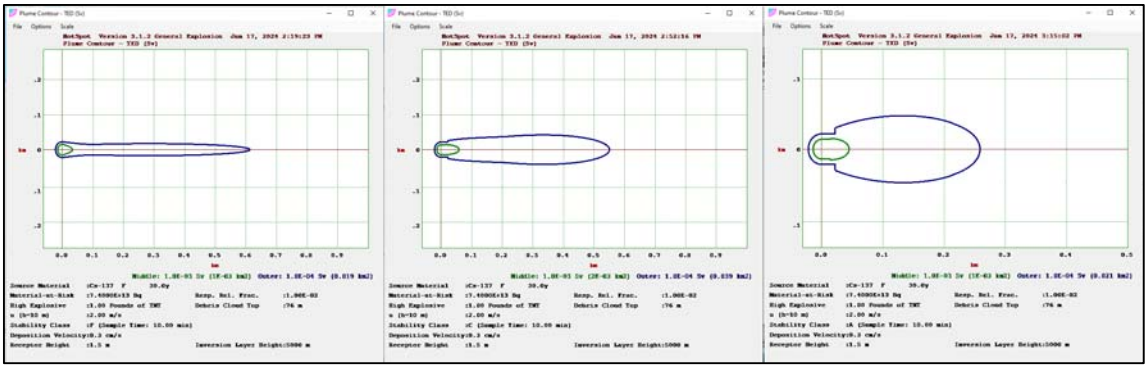

(a)

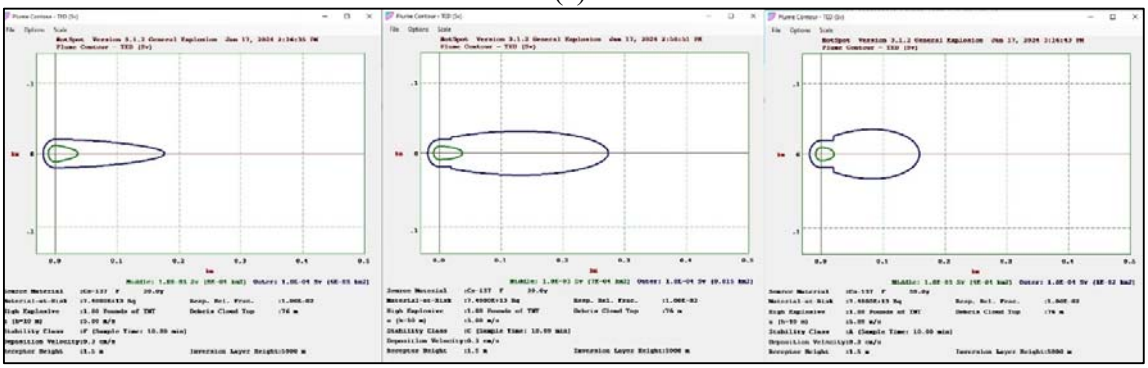

(b)

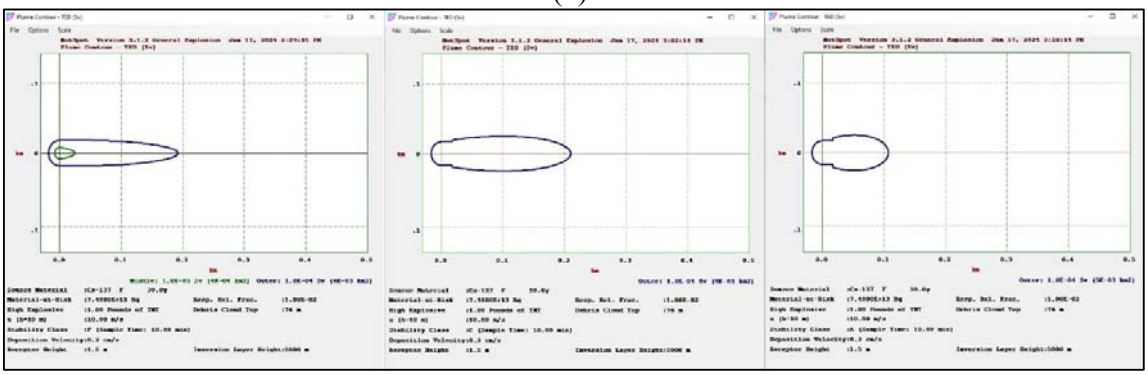

(c)

Figure 6. Mapping of TEDE as a function of wind speed for different atmospheric stability classes. (a), (b), and (c) show TEDE at wind speeds of 2 m/s, 5 m/s, and 10 m/s, respectively. From left to right, the maps represent stability classes F, C, and A.

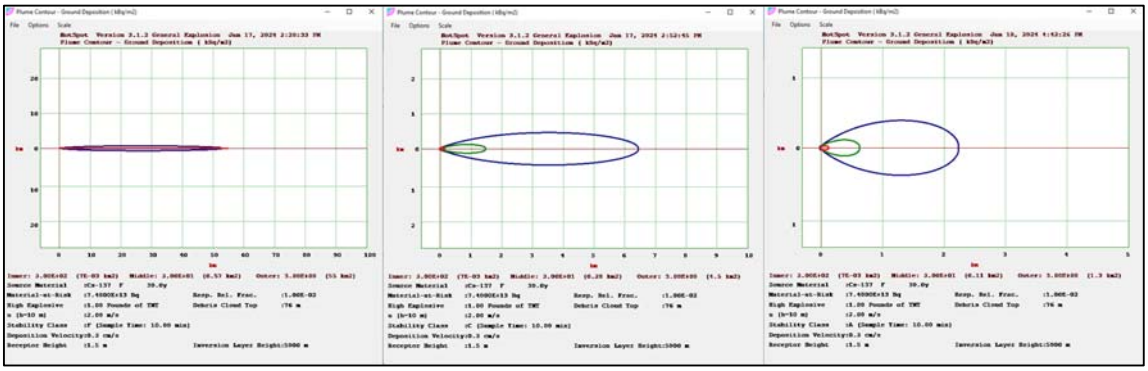

(a)

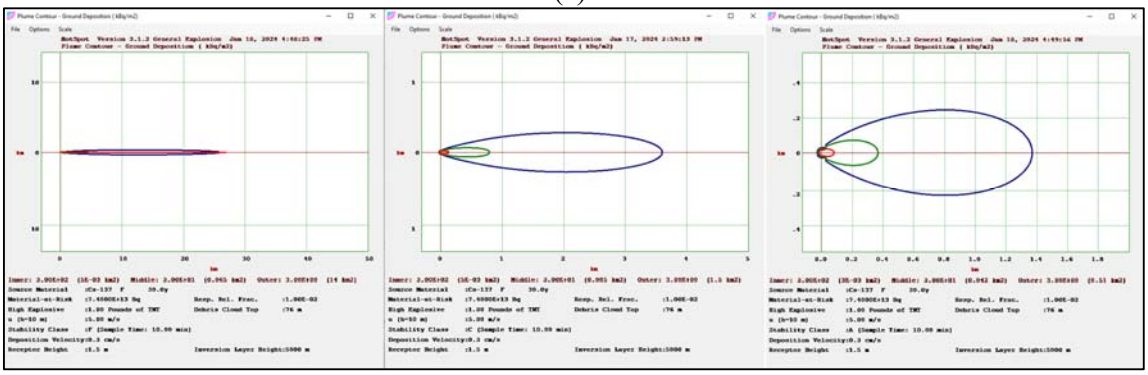

(b)

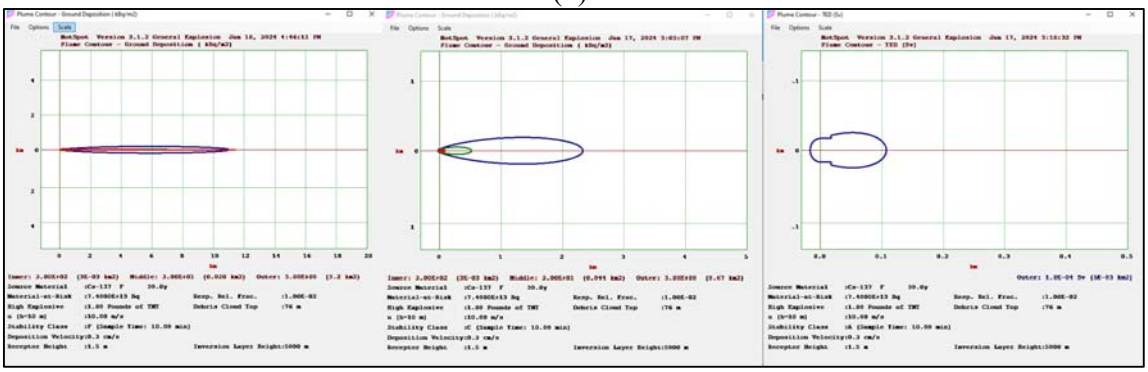

(c)

Figure 7. Ground deposition as a function of wind speed for different atmospheric stability classes. (a), (b), and (c) show TEDE at wind speeds of 2 m/s, 5 m/s, and 10 m/s, respectively. From left to right, the maps represent stability classes F, C, and A.

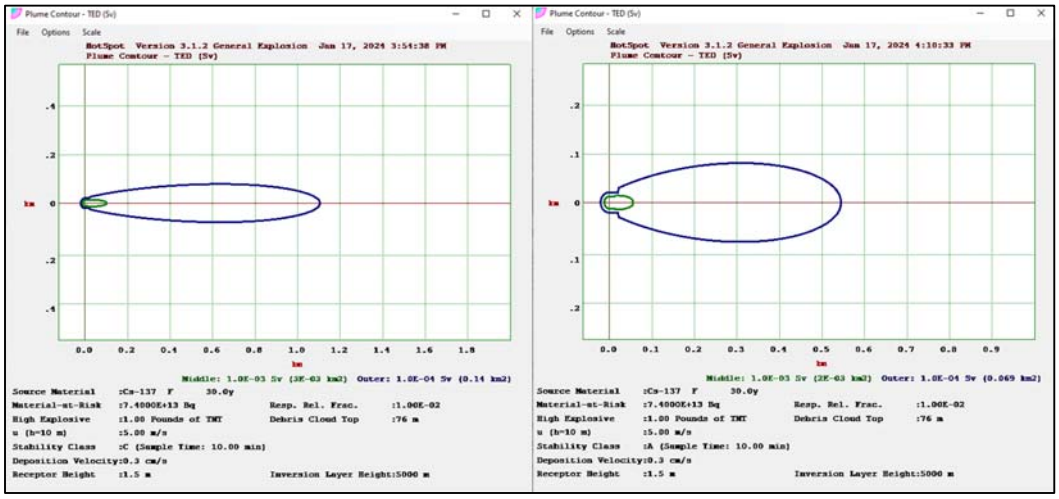

(a)

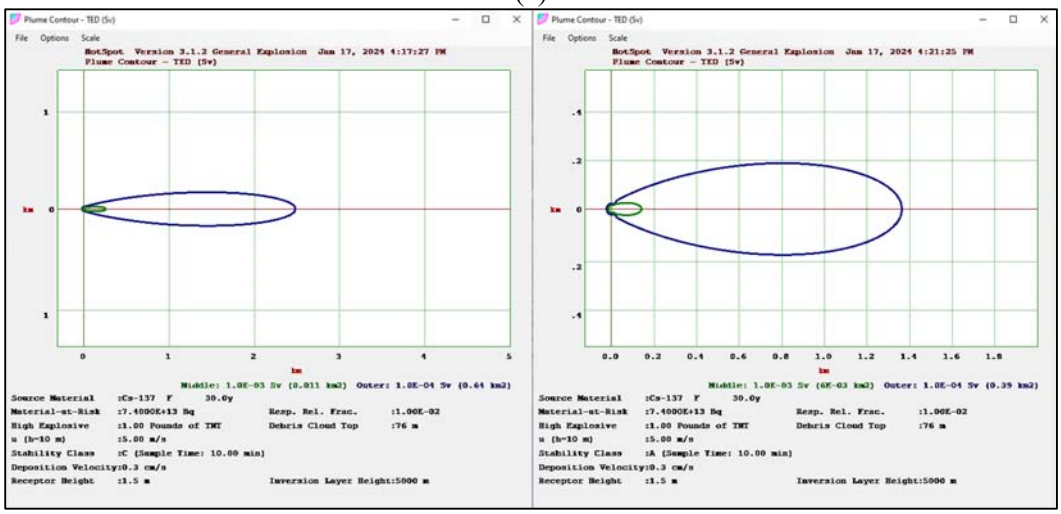

(b)

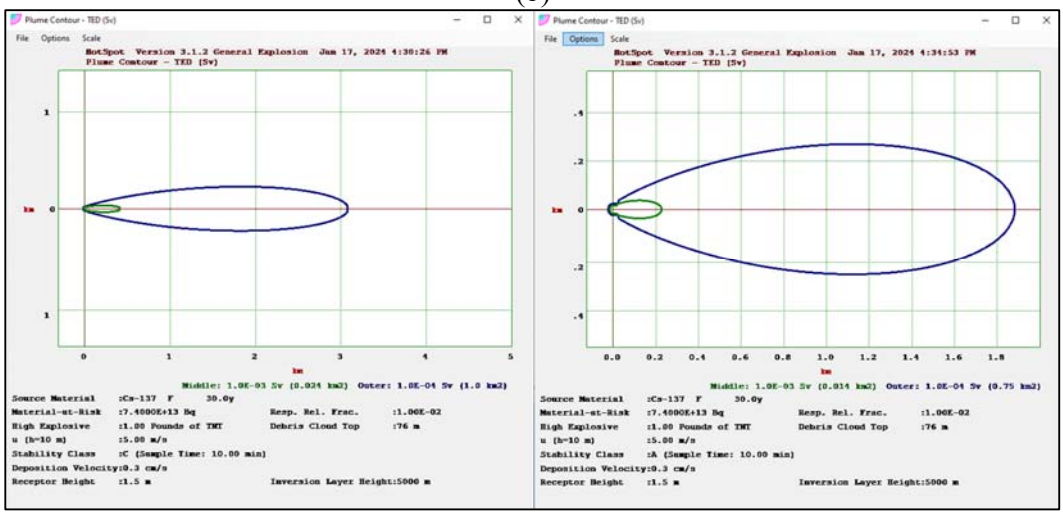

(c)

Figure 8. Mapping of TEDE as a function of precipitation for different atmospheric stability classes. (a), (b), and (c) show TEDE at precipitation of 1 mm/h, 5 mm/h, and 10 mm/h, respectively. From left to right, the maps represent stability classes F and A.

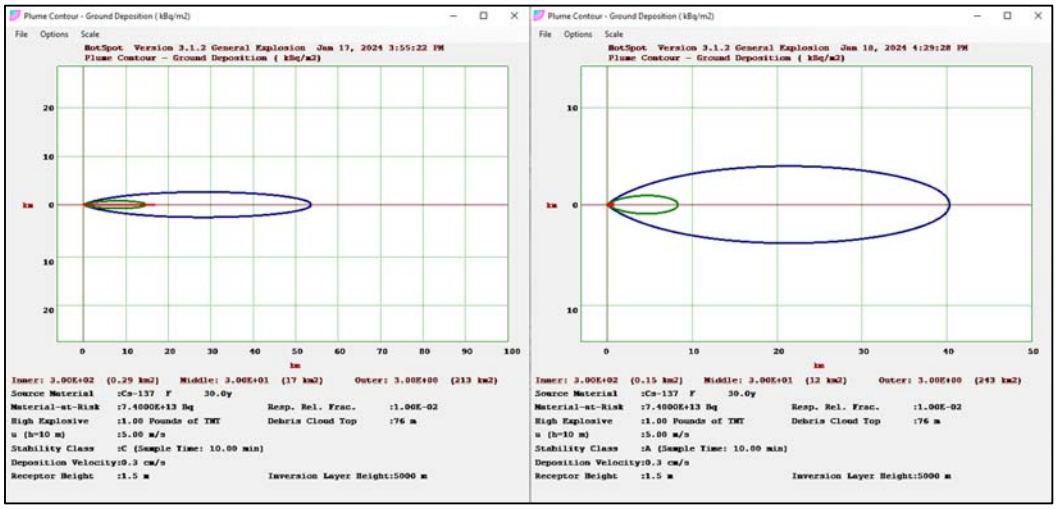

(a)

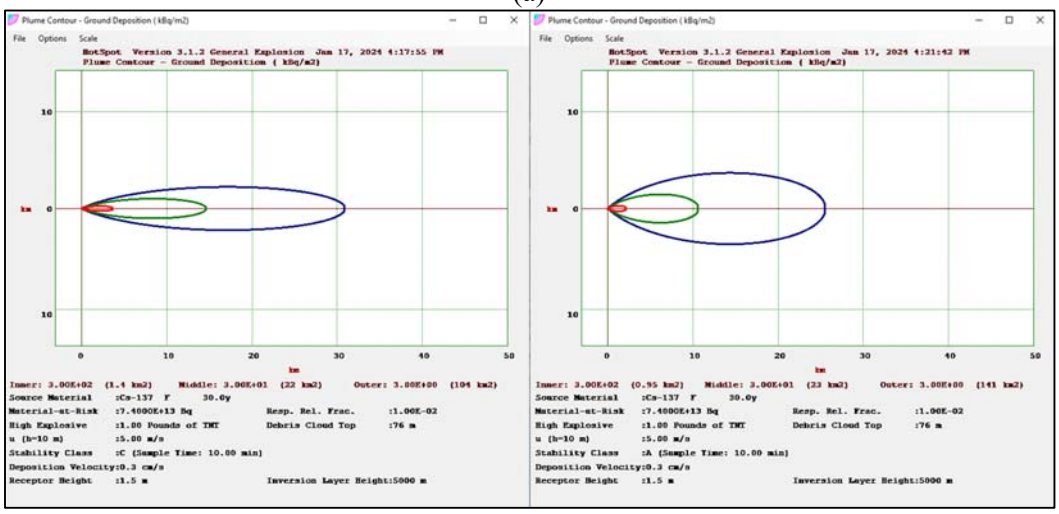

(b)

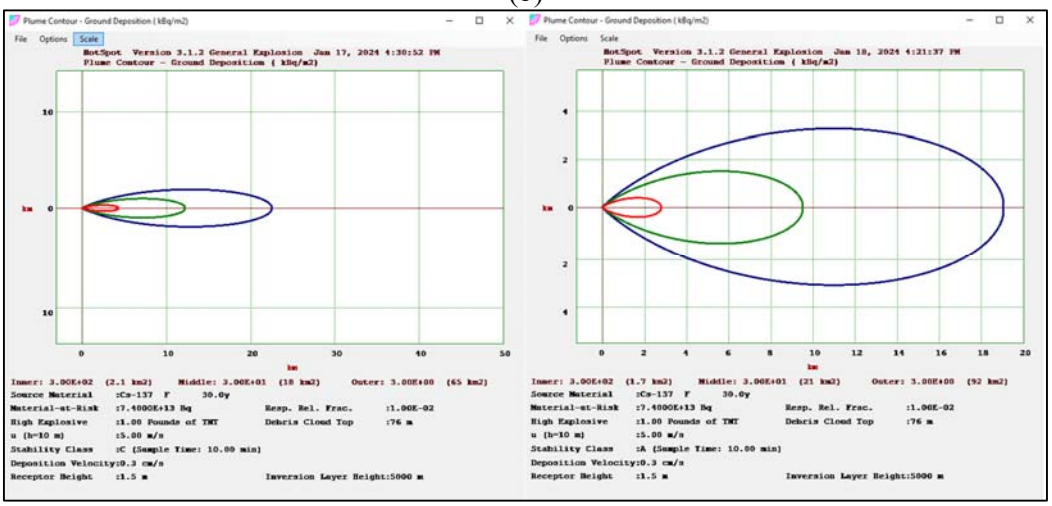

(c)

Figure 9. Ground deposition as a function of precipitation for different atmospheric stability classes. (a), (b), and (c) show TEDE at precipitation of 1 mm/h, 5 mm/h, and 10 mm/h, respectively. From left to right, the maps represent stability classes F and A.

Regarding the influence of precipitation, the results in Figures 8 and 9 indicate that in the presence of light rain (1 mm/h) with a medium wind speed of 5 m/s, the ground deposition area is significant. For example, in slightly unstable atmospheric conditions (class C) with a wind speed of 5 m/s, the red zone is 5E-3 km² and the green zone is 0.085 km² for a dry atmosphere. In case of light rain (1 mm/h), the red zone increases to 0.29 km² and the green zone reaches 17 km². In terms of TEDE, the green zone is 7E-4 km² for a dry atmosphere and 7E-3 km² in the presence of light rain (1 mm/h). The presence of heavy rain increases the TEDE contour, from 7E-3 km² in case of light rain (1 mm/h) to 0.024 km² in case of heavy rain (10 mm/h) when the atmosphere is slightly unstable (class C). The ground deposition area remains significant, reaching its maximum in the presence of rain (5 mm/h). In response to this situation, given that the scenario assumes the accident occurred near a stadium where many people are present during a match, measures must be taken. Supporters and residents in the green zone should be evacuated using transportation means such as buses and cars. The shelter is also possible in nearby buildings or evacuation into the forest. For areas where the dose is below 1 mSv and no intervention is needed, any unnecessary access to this area should be avoided. Emergency response teams can then implement their protection measures and provide the necessary responses. It is important to position them behind the release point relative to the wind direction. Analyzing the obtained results, it is clear that in the event of a scenario involving a dirty bomb, the results will vary depending on the weather conditions of the scenario. Therefore, the means to be deployed and the actions to be taken by national authorities will not be uniform.

4. Conclusions

Our study has elucidated the potential implications of a radioactive dispersion scenario involving a dirty bomb containing 74 TBq of Cs-137. We calculated the TEDE and ground deposition thresholds based on atmospheric stability classes, wind speed, and precipitation, revealing significant variability in outcomes depending on these parameters. The simulations demonstrated that atmospheric stability, wind speed, and precipitation critically influence the dispersion of the radioactive plume, the extent of ground deposition, and TEDE values. These findings highlight the necessity for meticulous planning of emergency measures tailored to the specific weather conditions of the scenario. In terms of response actions, our analysis offers clear recommendations for evacuating high-risk areas, sheltering affected individuals, and implementing protective measures for response teams. It is essential to consider dose levels, meteorological conditions, and local topography to effectively adapt intervention strategies.

Overall, this study underscores the importance of a comprehensive and adaptable approach to managing radiological incidents, emphasizing the need for robust emergency plans that consider the complexity of environmental factors affecting radioactive dispersion. Future studies will expand on this work by examining additional scenarios and varying conditions to further refine and improve emergency response strategies.

References

[1] C.D. Ferguson, Reducing the threat of RDDs, IAEA Bull. 45 (2003) 12–15.

[2] International Atomic Energy Agency, Implementing Guide IAEA Nuclear Security Series No. 11 Security of Radioactive Sources, 2009.

[3] A. Chetaine, O. Kabach, S. Abdelmajid, ASSESSMENT METHODOLOGIES AND EVALUATION OF THE PHYSICAL PROTECTION SYSTEM, in: Int. Conf. Phys. Prot. Nucl. Mater. …, 2018: pp. 1–8.

[4] O. Kabach, A. Chetaine, A. Benchrif, Physical Protection System, Corrective Actions, and Weaknesses Identification Based on Nuclear Security Series: The Hypothetical Atomic Research Institute (HARI) Case, Int. J. Nucl. Secur. 6 (2020). https://doi.org/10.7290/ijns060104.

[5] A. Rump, S. Eder, C. Hermann, A. Lamkowski, P. Ostheim, M. Abend, M. Port, Estimation of radiation-induced health hazards from a "dirty bomb" attack with radiocesium under different assault and rescue conditions, Mil. Med. Res. 8 (2021) 1–20. https://doi.org/10.1186/s40779-021-00349-w.

[6] D. Haranger, La personne compétente en radioprotection, Rev. Générale Nucléaire (2002) 67–68. https://doi.org/10.1051/rgn/20022067.

[7] C.A. Margeanu, EG1100484 Comparative Study on Radiological Impact due to Direct Exposure to a Radiological Dispersal Device using a Sealed Radiation Source, (2010) 27–30.

[8] K.M. Thiessen, P. Kuca, J. Helebrant, J. Hulka, T.W. Charnock, S.L. Chouhan, J. Duran, V. Fuka, G. De With, F. Mancini, R. Perianez, B.K. Tay, D. Trifunovic, H. Walter, Modelling the atmospheric dispersion of radiotracers in small-scale, controlled detonations: Validation of dispersion models using field test data, J. Radiol. Prot. 42 (2022). https://doi.org/10.1088/1361-6498/ac66a2.

[9] M.A. Al-Aqeel, I.A. Alrammah, Radiological Impact Assessment for hypothetical accident scenarios of a proposed pressurized water reactor using HotSpot code, Radiat. Phys. Chem. 204 (2023) 110717. https://doi.org/10.1016/j.radphyschem.2022.110717.

[10] D. Kundu, C. V. Srinivas, S. Chandrasekaran, B. Venkatraman, Radiological consequence assessment for hypothetical nuclear explosion scenario using HotSpot, Prog. Nucl. Energy 147 (2022). https://doi.org/10.1016/j.pnucene.2022.104192.

[11] J.F. Pereira, J.U. Delgado, Dirty bomb radiological simulations: two explosion scenarios using the Rio 2016 Olympic games Athletes' Village as a model, Brazilian J. Radiat. Sci. 6 (2018) 1–18. https://doi.org/10.15392/bjrs.v6i2.345.

[12] U.S. Department of Health & Human Services, Radiological Dispersal Devices (RDDs), (2024). https://remm.hhs.gov/rdd.htm (accessed January 11, 2024).

[13] F.D. Sowby, Editorial Board, Ann. ICRP 6 (1981) IFC-IFC. https://doi.org/10.1016/0146-6453(81)90127-5.

[14] BELHAJ Boubker, Etude de la dispersion d'un nuage radioactif en vue d'optimiser I'intervention en cas d'urgence radiologique et nucléaire, Ibn Tofail university, 2015.

[15] S.G. Homann, F. Aluzzi, HotSpot Health Physics Codes Version 3.1.2 User's Guide, 2010. https://www.osti.gov/biblio/1231323.

[16] Windfinder, Statistiques annuelles des vents et de la météo pour Kenitra Air Base, (2024). https://fr.windfinder.com/windstatistics/kenitra (accessed January 1, 2024).